Nanoparticles of $CdCl_2$ with Closed Cage Structures

RONIT POPOVITZ-BIRO, ANTON TWERSKY, YARON ROSENFELD HACOHEN, AND RESHEF TENNE*
Department of Materials and Interfaces, The Weizmann Institute of Science, Rehovot 76100, Israel

(Received 21 June 2000)

Abstract. Nanoparticles of various layered compounds having a closed cage or nanotubular structure, designated also inorganic fullerene-like (*IF*) materials, have been reported in the past. In this work *IF*-$CdCl_2$ nanoparticles were synthesized by two methods. In one technique, a high temperature evaporation and subsequent condensation of dried cadmium chloride powder was used. In the other method, electron beam irradiation of the source powder led to its recrystallization into closed nanoparticles with a nonhollow core. The two methods are shown to produce nanoparticles of different topologies. While mostly spherical nested structures are obtained from the high temperature process, polyhedra with hexagonal or elongated rectangular characters are obtained by the electron beam induced process. The analysis also shows that, while the source (dried) powder is orthorhombic cadmium chloride monohydrate, the crystallized *IF* cage consists of the anhydrous 3R polytype which is not stable as bulk material in ambient atmosphere. Consistent with previous observations, this study shows that the seamless structure of the *IF* materials can stabilize phases, which are otherwise unstable in ambient conditions.

INTRODUCTION

Graphite nanoparticles were shown to be unstable in the planar form and undergo a spontaneous morphological transformation that causes them to curl up into nanoballs (fullerenes)[1] or nanotubes.[2] The stimulus for this morphological change is the decrease in the size of one such layer, which increases the ratio between the dangling bonds at the periphery of the layer and the number of atoms within the layer (bulk). The larger the ratio, the greater the instability due to the high surface energy and therefore the propensity to form hollow cage structures. Disposing pentagons into the otherwise hexagonal network imposes curvature into the layer. Thereby, the layer is able to close on itself and eliminate the dangling bonds. This curvature causes stress in the layer, due to the deviation of the sp^2 bonds from planarity. The elastic stress energy is nonetheless more than compensated by elimination of the dangling bonds. Therefore the total energy of the closed cage nanostructures is reduced relative to the planar form of graphite. However, large energy input is required in order to initiate this folding process, which explains the need for the high temperatures or other energy sources, in order to produce carbon fullerenes and nanotubes.

The research into C_{60} and related structures, like nanotubes, paved the way for the discovery of such morphologies in other layered materials, such as MS_2[3–5] (M = Mo,W, etc.), other chalcagonides,[6,7] BN,[8] halides,[9] oxides,[10–12] and others. They were all found to create inorganic fullerene-like (IF) structures in a manner analogous to carbon. The structures of the layered compounds are more complicated than the simple hexagonal structure of graphite sheets, and therefore the stress relief mechanism is more complicated too. Although *IF* of certain metal chalcagonides have been relatively thoroughly investigated,[3–5] their stress relief structure is not yet fully understood. In this respect, it was proposed, that triangles and squares (rectangles), rather than pentagons, would be preferred as the lower symmetry element, which is responsible for the curvature of the *IF* structures. This hypothesis was confirmed in recent studies of both MoS_2 and BN. Thus, MoS_2 polyhedra with octahedral structure were recently synthesized.[13] In another recent study, MoS_2 nanotubes with either three rectangles or one octagon and four rectangles (negative curvature) in their cap, were proposed to be stable struc-

*Author to whom correspondence should be addressed. E-mail: cpreshef@weizmann.ac.il

tures.[14] *IF* structures of boronitride were shown[15,16] to contain B_2N_2 squares, rather than pentagons, which are typical of carbon fullerenes and nanotubes. MoS_2 crystallizes in a trigonal prismatic structure (2H), which is not likely to form octahedral polyhedra easily, but has a metastable tetragonal phase (1T) with Mo in octahedral coordination.[17] On the other hand, $CdCl_2$ crystallizes in a hexagonal lattice in which each Cd atom is surrounded by 6 Cl atoms in an octahedral coordination.[18] It was hypothesized that the octahedral environment of Cd in $CdCl_2$ will facilitate the formation of *IF* moieties with octahedral shape. In addition, *IF*-$CdCl_2$ can theoretically be made by pure evaporation/condensation process at 750 °C, which was thought to be a good practice to obtain nanoparticles with closed cage structure. Previous work on the synthesis of closed cage (fullerene-like) structures of $NiCl_2$ revealed three typical topologies:[9] multilayer (onion) nanoparticles of a spherical shape, multilayer nanotubes, and closed cage structures with hexagonal topology. The first two kinds of structures were observed before, while the hexagonal topology was unique to this compound. Since $NiCl_2$ crystallizes in the cadmium chloride (layered) structure, it was interesting to know if this latter topology is common to other materials with cadmium chloride structures, like $CdCl_2$ itself.

The $CdCl_2$ structure is made of a staggered stacking of three Cl-Cd-Cl layers having interlayer distance (C/3) of 0.58 nm and a rhombohedral unit cell (3R) (Space group *R3m*),[19] as shown in Fig.1a. The crystal of $CdCl_2$ is not stable in the ambient atmosphere. Like many other layered compounds, especially the more ionic ones like those containing halides, facile water intercalation into the van der Waals gaps occurs through the prismatic edges. It absorbs first one water molecule and transforms readily into the monohydrate ($CdCl_2.H_2O$). The monohydrate is also a layered compound that packs in an orthorhombic space group (*Pnma*)[20] as shown in Fig. 1b, with layer to layer distance of 0.59 nm (C/2). In this structure one water molecule replaces a chlorine atom and therefore each Cd atom is surrounded by 5 Cl atoms and one oxygen atom, with the hydrogen atom pointing out into the van der Waals gap, forming a hydrogen bond between two of the oxygen atoms of

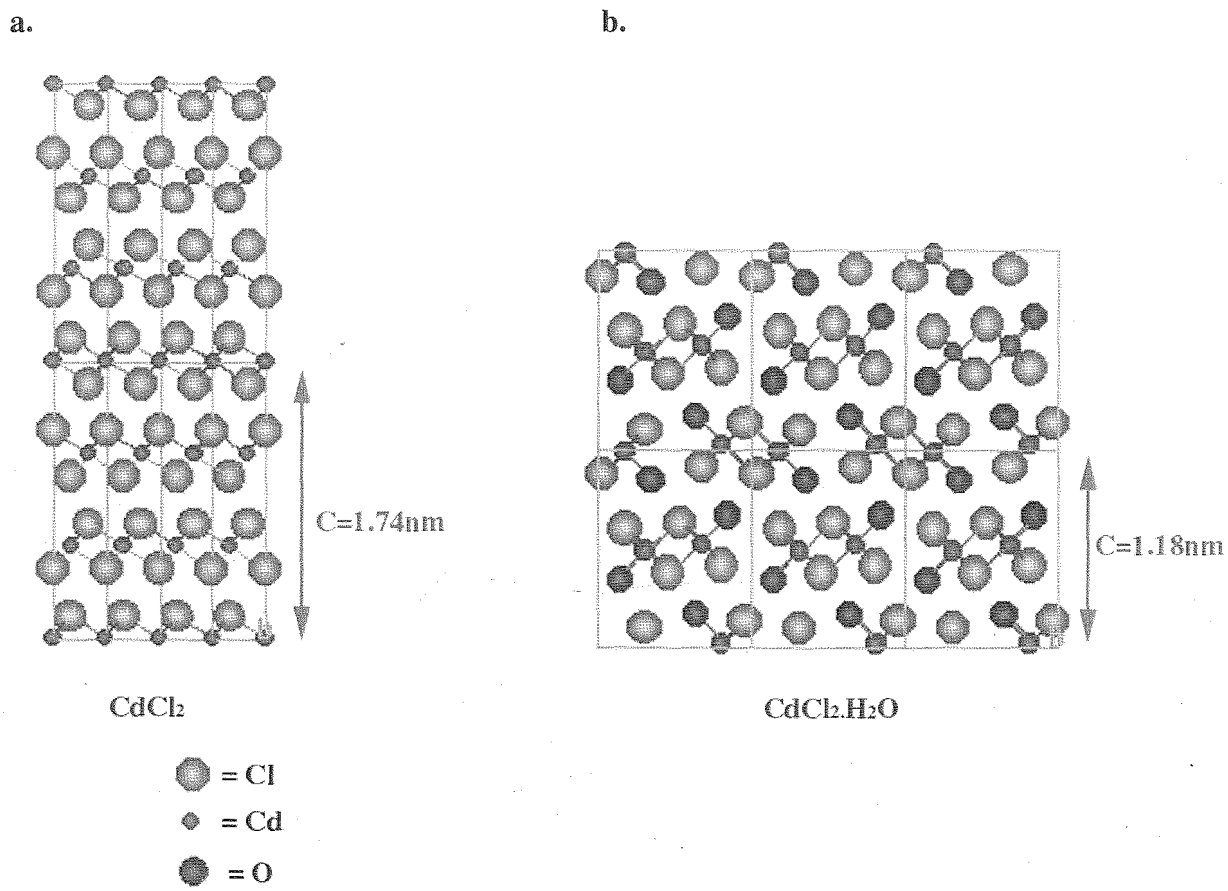

Fig. 1. Schematic illustration of the crystal structure of (a) $CdCl_2$ and (b) $CdCl_2.H_2O$, both shown in the (010) projection.

neighboring layers. Absorption of water through intercalation into the van der Waals gap of the layered monohydrate can lead to its exfoliation and eventually to dissolution of the salt by the self-absorbed water molecules. On the other hand, $CdCl_2$ containing more than one molecule of water, like $CdCl_2 \cdot 2.5H_2O$, is known.[21] In this crystal, the cadmium atoms are octahedrally coordinated, and the octahedra are tightly bound together through hydrogen bonds. They are sensitive to the ambient atmosphere and therefore cannot be studied in the air. Furthermore, absorption of water leads to the formation of higher hydrates and to the self dissolution of the salt in the absorbed water molecules. These chemical and structural changes explain the great difficulties encountered during the present study.

EXPERIMENTAL METHODS

A setup for evaporation of $CdCl_2$ and its controlled condensation was constructed. The main system used is illustrated in Fig. 2. It consists of a quartz tube (reactor) inserted into a horizontal oven. This reactor was connected to a closed gas system that permitted the use of different atmospheres [Ar, forming gas (5% H_2 ; 95% N_2), chlorine]. Into this reactor an additional quartz pipe was inserted with one end open and the other partially closed. A crucible, with 0.25–0.3 g of pre-dried $CdCl_2$ (dried by heating to 200 °C), was inserted (by magnet) into the inner pipe in the center of the oven and heated to temperatures ranging from 600 to 800 °C. The material was evaporated and carried by the carrier gas to the end of the inner pipe, out of the oven, where it condensed and was collected after cooling. The collected powdered material was examined by X-ray diffraction (XRD). It was found that the majority phase in the powder was indeed $CdCl_2 \cdot H_2O$ in all cases. The powder was also suspended in ethanol or CCl_4 and was dripped onto a Cu grid and studied by transmission electron microscopy (TEM) (Philips EM400 and CM120, both operating at 120 kV). Various oven temperatures, gas flow speeds and atmospheres were tried, with the best results obtained under the flow of Ar at a rate of 55 cm^3/min and a temperature of 750 °C.

A few alternative synthetic approaches have been pursued, but none of them yielded cage structures of $CdCl_2$ in a reproducible manner. However, it was found that irradiation of the cadmium chloride monohydrate powder by the electron beam of the Philips CM120 TEM for approximately 15 min led to a recrystallization and produced cage structures, as reported below.

RESULTS AND DISCUSSION

Figure 3 shows an assortment of *IF*-$CdCl_2$ nanoparticles produced by the evaporation/condensation method at 750 °C. Some of the nanoparticles were fully nested fullerene-like structures, approximately 30 layers thick, while the others had only 15–20 closed layers. The nature of the core is uncertain; it could be either hollow or consist of amorphous cadmium chloride. Unfortunately, this and a few other related procedures which have been attempted, could not lead to reproducible formation of closed cage structures of $CdCl_2$. Regrettably, this is not an uncommon situation in the synthesis of fullerene-like materials. Most disturbing is the fact that the monohydrate is very stable at ambient conditions, and so even after a high-temperature annealing process and subsequent cooling, the XRD of the product was always dominated by this material. Furthermore, the product was not stable under electron beam irradiation during TEM analysis. This difficulty probably stems from the fact that the monohydrate is hygroscopic and out-gassing of the water molecules during the analysis did not permit the search for the (anhydrous) nanoparticles.

More careful observation under the electron microscope was done on a preheated $CdCl_2$ material. According to XRD and electron diffraction (ED) analyses, the precursor consists mostly of $CdCl_2 \cdot H_2O$, which trans-

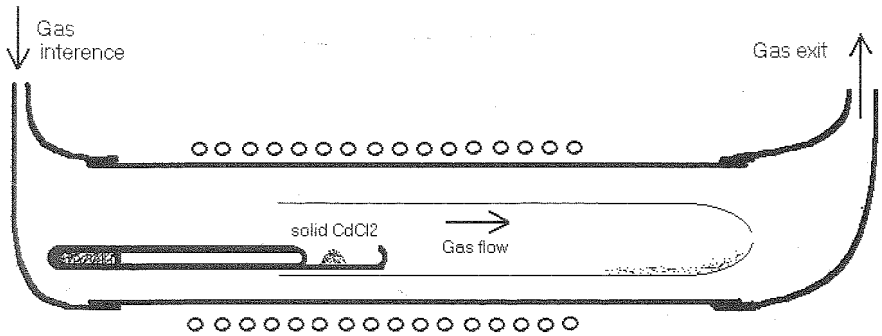

Fig. 2. Schematic illustration of the apparatus used for the synthesis of *IF*-$CdCl_2$ structures by evaporation/condensation method.

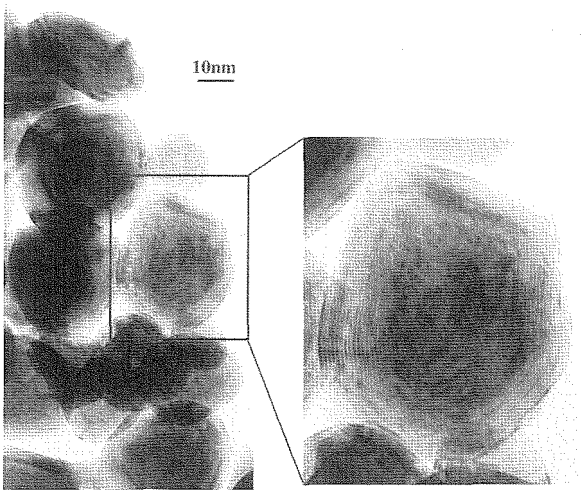

Fig. 3. TEM micrograph of multi-layer *IF*-$CdCl_2$ structures, synthesized by evaporation/condensation method. The distance between the $CdCl_2$ layers (fringes) is 0.58 nm.

forms in situ under the electron beam irradiation into *IF*-$CdCl_2$ nanoparticles, i.e., closed cage structures of the anhydrous 3R-$CdCl_2$. This chemical and structural transformation is demonstrated in the TEM micrographs shown in Figs. 4 and 5. The low-magnification images in Fig. 4 show that under the e-beam irradiation, the macroscopic particle of the monohydrate breaks down and recrystallizes into new nanoparticles. The ED pattern of the particle changes during exposure to the beam, from single crystal to a powder pattern with residual preferred orientation (Fig. 4). The structural and chemical transformation is further elucidated using selected area electron diffraction from a 80×80 nm^2 region and high-resolution imaging of this domain (Fig. 5). Although a large number of nanocrystals contribute to the electron diffraction, the arc pattern with sixfold symmetry indicates that the crystals are arranged in a preferred orientation. The diffraction spots could be assigned and attributed to the anhydrous 3R-$CdCl_2$ polymorph. Thus, the closed cage structures were formed by release of the water molecules from the monohydrate crystal and subsequent crystallization into the anhydrous form. Closer examination of the nanoparticles shows that most of the nanoparticles have a core-shell structure with a closed cage $CdCl_2$ shell and an amorphous core of an unspecified chemical composition. This is not an uncommon situation and has been observed before in, e.g., the recrystallization of amorphous MoS_3 nanoparticles. After exposure to the e-beam irradiation[7] or pulsed electric signal,[6] core-shell structures with MoS_2 shell and amorphous MoS_3 core have been formed. In both cases the core remains amorphous, since its recrystallization requires an out-diffusion of molecules through the already formed closed shell. In the present case, out-diffusion of the water molecules through the *IF*-$CdCl_2$ shell is rather

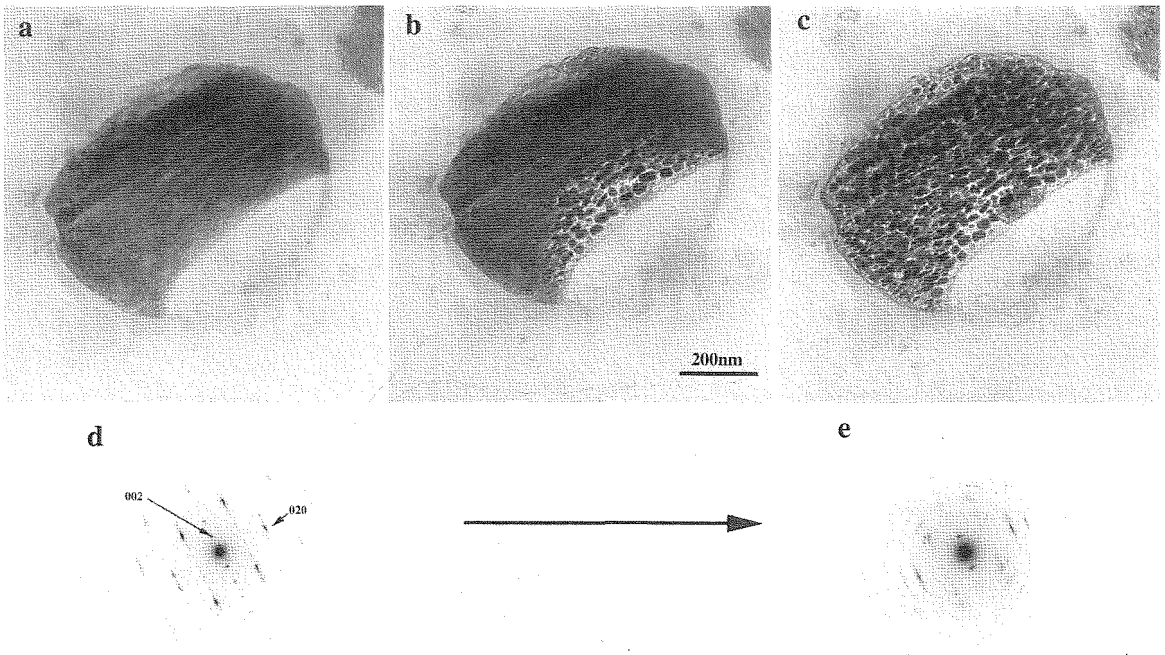

Fig. 4. TEM micrographs showing the transformation of (a) single $CdCl_2 \cdot H_2O$ particle into (c) nanoparticles of $CdCl_2$ with closed cage structures, under e-beam irradiation. Electron diffraction of (d) the precursor and (e) the product are also shown.

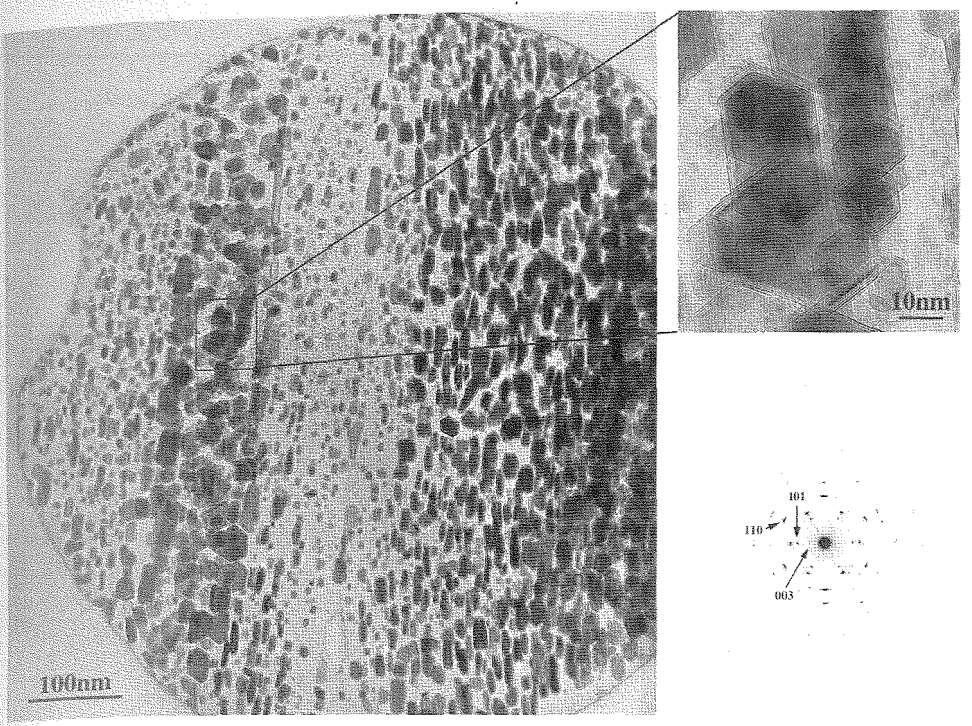

Fig. 5. TEM micrograph showing $CdCl_2$ particles formed under e-beam irradiation. On the right are shown a magnified region and, below it, its electron diffraction pattern, exhibiting the hexagonal symmetry of the 3R-$CdCl_2$ polytype.

slow, once the first few layers of the shell are formed.

Figures 6–8 show a few typical structures obtained after electron beam irradiation with 120 keV for approximately 15 min. Thus Fig. 6 shows an almost perfect hexagonal cage structure with sharp 120° inclinations. The distance between the fringes (0.58 nm) agrees with the C/3 distance between the $CdCl_2$ layers. Figure 7 shows an image and electron diffraction of another hexagonal cage structure which was obtained by the same method. Upon tilting the sample by 20°, four oppositely placed walls of the cage have disappeared, while two walls remained in focus. This picture indicates that the walls which have disappeared are inclined in very sharp angles to the beam. This observation entails that the present cage structure of $CdCl_2$ is a rhomboid with some very sharp angles. The diffraction pattern contains superposition of spots from both the {003} and {hk0} planes, which indicates that the two types of planes are parallel to the beam, i.e., the nanostructure constitutes a closed cage structure. In addition to the diffraction spots, three rings were obtained which could be assigned to 002, 101, and 103 reflections from elemental cadmium, perhaps formed by loss of Cl atoms and residing in the background. Figure 8 shows a few typical cage structures, which are mostly typified by 120° inclinations on one hand and 90° inclinations on the other hand. In many cases the rectangles possess a rather elongated shape. It is believed that the hexagonal (Fig. 8a) and rectangular (Fig. 8b) images are characteristic projections of similar cages taken at two perpendicular angles. Since the maximum tilting angle of the sample in the microscope is ±40°, it is not possible to tilt the same polyhedron from one projection to the other. Apparently, the cage structures are disposed on the substrate in two preferred orientations, either with their hexagonal or with their rectangular faces parallel to the substrate. Figure 9 shows a view of a rhombic cage motif in two projections, 90° with respect to each other. It is clear from this figure, that in order to transpose the

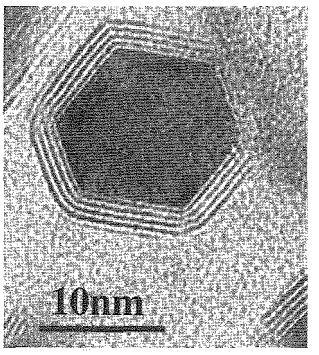

Fig. 6. TEM micrograph showing a $CdCl_2$ cage structure with four layers in the shell and hexagonal morphology.

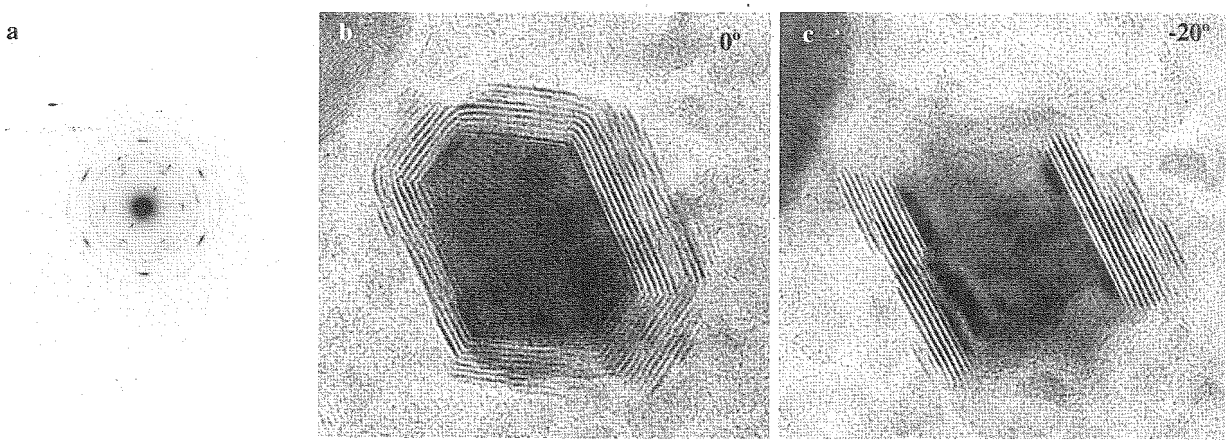

Fig. 7. Selected area electron diffraction (a) and image of a $CdCl_2$ cage, shown at (b) 0° and (c) 20° tilt.

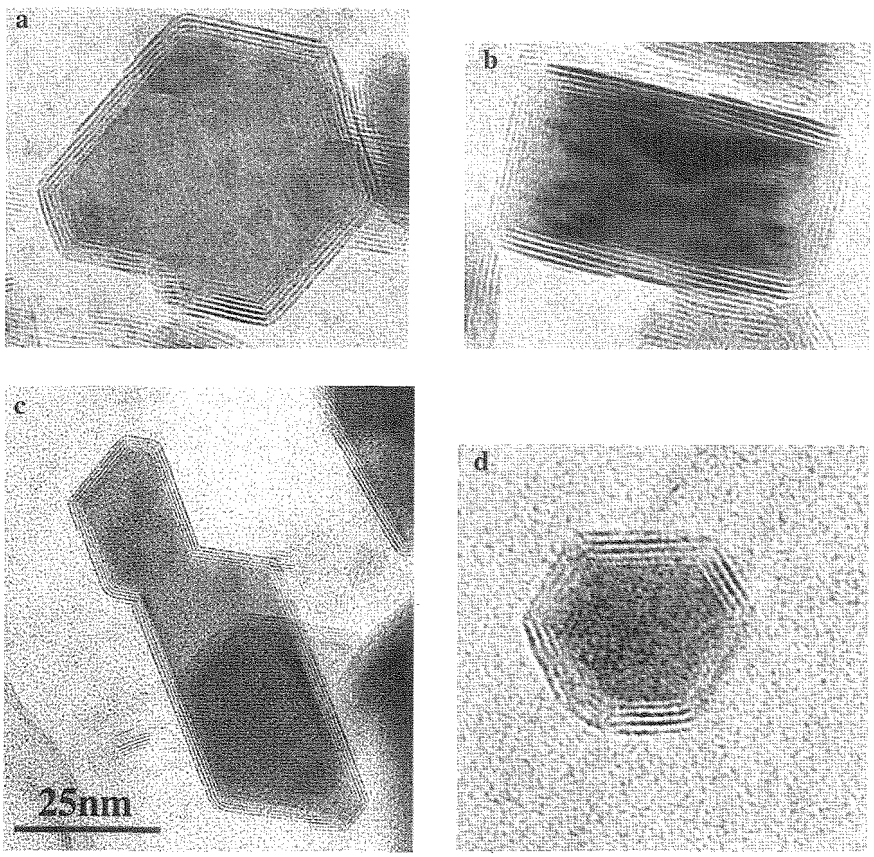

Fig. 8. TEM micrographs showing an assortment of $CdCl_2$ cage structures with hexagonal or rectangular shapes. The distance between the $CdCl_2$ layers (fringes) is 0.58 nm.

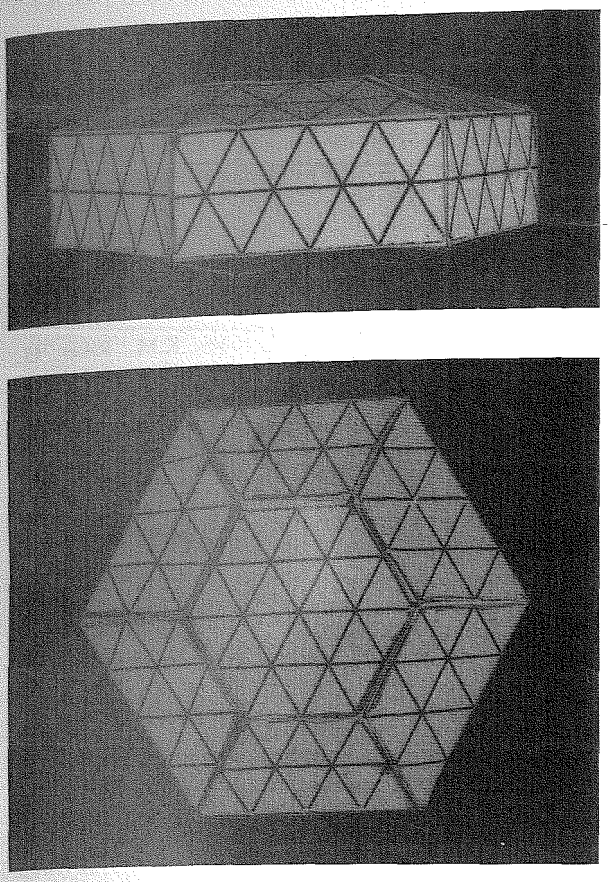

Fig. 9. A rhombic cage model shown in two projections, 90° with respect to each other.

structure from, e.g., the hexagonal projection to the rectangular, it is necessary to tilt the sample by 90°. It is also clear that tilting a similar multilayer cage structure of $CdCl_2$ in all the intermediate angles will result in a disappearance of some of the planes, while others will remain in focus, as indeed has been observed (see, for example, Fig. 7). Hexagonal cage structures were previously observed in *IF*-$NiCl_2$, which crystallizes also in the cadmium chloride structure.[9] This fact lends support to the idea that nanoparticles of layered compounds with octahedral coordination tend to form cage structures with hexagonal shape, rather than the initially hypothesized octahedral polyhedra.

It has been pointed out before[6,7,12] that phases that are not stable in the bulk can nonetheless form metastable *IF* structures. In that sense, the present case is not an exception. It is quite unexpected, however, that while bulk 3R-$CdCl_2$ is hygroscopic, and therefore cannot be studied in ambient conditions, *IF* structures of the same compound are fully stable in the ambient.

This work reveals another important attribute of closed cage nanostructures. As discussed in the previous section, fullerene-like structures can be spontaneously formed by heating nanoparticles of layered materials. The energy input is required to start the folding process, which is stimulated by the introduction of pentagons, squares, or triangles into the otherwise hexagonal array. Many of the compounds which form the closed structures, like $CdCl_2$, are unstable in ambient conditions. Therefore the formation of the closed *IF* nanostructures can be considered as a means to stabilize high-temperature phases. Obviously, mono (and higher) hydrates of $CdCl_2$ are unstable at elevated temperatures. Accordingly, the thermodynamically stable phase at high temperatures is the anhydrous $CdCl_2$. This high-temperature phase can be made fully stable at ambient conditions only in the seamless *IF* structure, which prevents water intercalation. This observation is by no means limited to this case, as has been shown for various other phases, like metal intercalated MoS_2[6,7,22] or Tl_2O[12] and others.

The continuum theory, which takes into account the elastic energy of bending of the atomic layers together with the energy for introducing dislocations (grain boundaries), and the surface energy of the nanoparticles, has been used to calculate the stable structure of the closed MoS_2 nanoparticles.[23] This theory predicts that the first layer or two of the nanoparticles can bend rather uniformly, leading to quasi-spherical nanoparticles. However, when the ratio of the thickness of the nanoparticle wall to its radius increases beyond a certain value (ca. 0.1), the bending energy becomes too large to afford a uniform bending, and a phase transition into a polyhedral structure is obtained. For nanoparticles of a radius 30–50 nm a kink is therefore predicted for a number of layers exceeding 5–7. This result is corroborated by the results of the synthesis of fullerene-like WS_2 (MoS_2) nanoparticles.[24,25] Similar transformations are anticipated and indeed observed for the synthesis of *IF*-$CdCl_2$ through a high-temperature sublimation/condensation reaction (see Fig. 3). Obviously, the bending energy of one-dimensional objects, like the nanotubes, is appreciably smaller, and therefore polygonal multiwall WS_2 nanotubes are rather rare.

Electron beam induced synthesis of nested carbon fullerenes was beautifully demonstrated by Ugarte,[26] and later on by Banhart.[27] Electron beam irradiation of hexagonal boron nitride resulted in octahedral BN onions.[16] A similar method was used to synthesize nested MoS_2[28] and WS_2[29] fullerene-like nanostructures. One of the main differences between the high temperature and electron beam induced synthetic approaches is that in the first, the entire reactor is heated and consequently the gaseous phase is in equilibrium with the solid phase. Therefore, comparison between predictions made through theory and the experimental work is feasible.

This is not necessarily the case for electron beam induced synthesis of the fullerene-like nanostructures. The high-energy deposition by the electron beam leads to a strong local heating of the solid, which can induce very fast diffusion of the species, locally. This effect can lead to a very fast healing of defects in the nanostructures. This is supported by the calculations of Bates and Scuseria,[30] who envisage a fast healing of defects in irradiated nested carbon fullerenes via a heptagon–pentagon carbon pair formation. However, frequently the rapid growth induced by the electron beam does not lend itself to the formation of defect-free structures, and many edge dislocations can be discerned in the nested nanostructures. Obviously this is not always the case in the present study, as shown for example in Figs. 5–7.

The most important issue, which remains unresolved so far, is the molecular structure of the rhombi corners. According to the Euler rule, 6 squares are required to close the otherwise hexagonal arrangement of the Cd (Cl) atoms in the layer plane. However, according to the present model, the $CdCl_2$ cage consists of 12 corners, which could be formed by pentagons, only. Further work is necessary to elucidate this important issue.

Acknowledgments. This work was carried out with the support of the Alfried Krupp von Bohlen and Halbach Stiftung (Germany), ACS-PRF (USA), AFIRST (France-Israel), Israel Academy of Sciences (Bikura), United States-Israel Binational Science Foundation, and the Israel Science Foundation.

REFERENCES AND NOTES

(1) Kroto, H.W.; Heath, J.R.; O'Brien, S.C.; Curl, R.F.; Smalley, R.E. *Nature* **1985**, *318*, 162–163.
(2) Iijima, S. *Nature* **1991**, *354*, 56–58.
(3) Tenne, R.; Margulis, L.; Genut, M.; Hodes, G. *Nature* **1992**, *360*, 444–446.
(4) Margulis, L.; Salitra, G.; Tenne, R.; Talianker, M. *Nature* **1993**, *365*, 113–114.
(5) Feldman, Y.; Wasserman, E.; Srolovitz, D.A.; Tenne, R. *Science* **1995**, *267*, 222–225.
(6) Homyonfer, M.; Alperson, B.; Rosenberg, Y.; Sapir, L.; Cohen, S.R.; Hodes; G., Tenne, R. *J. Am. Chem. Soc.* **1997**, *119*, 2693–2698.
(7) Hershfinkel, M.; Gheber, L.A.; Volterra, V.; Hutchinson, J.L.; Margulis; L.; Tenne, R. *J. Am. Chem. Soc.* **1994**, *116*, 1914–1917.
(8) Chopra, N.G.; Luyken, J.; Cherry, K.; Crespi, V.H.; Cohen, M.L.; Louie, S.G.; Zettl, A. *Science* **1995**, *269*, 966–967.
(9) Rosenfeld Hacohen, Y.; Grunbaum, E.; Tenne, R.; Sloan, J.; Hutchinson, J.L. *Nature* **1998**, *395*, 336.
(10) Spahr, M.E.; Bitterli, P.; Nesper, R. *Angew. Chem., Int. Ed. Engl.* **1998**, *37*, 1263–1265.
(11) Avivi, S.; Mastai, Y.; Hodes, G.; Gedanken, A. *J. Am. Chem. Soc.* **1999**, *121*, 4196–4199.
(12) Avivi, S.; Mastai, Y.; Gedanken, A. *J. Am. Chem. Soc.* **2000**, *122*, 4331–4334.
(13) Parilla, P.A.; Dillon, A.C.; Jones, K.M.; Riker, G.; Schulz, D.L.; Ginley; D.S.; Heben, M.J. *Nature* **1999**, *397*, 114.
(14) Seifert, G.; Terrones, H.; Terrones, M.; Jungnickel, G., Frauenheim, T. *Phys. Rev. Lett.* **2000**, *85*, 146–149.
(15) Terrones, M.; Hsu, W.K.; Terrones, H.; Zhang, J.P.; Ramos, S.; Hare, J.P.; Castillo, R.; Prassides, K.; Cheetham, A.K.; Kroto, H.W.; Walton, D.R.M. *Chem. Phys. Lett.* **1996**, *259*, 568–573.
(16) Golberg, D.; Bando, Y.; Stephan, O.; Kurashima, K. *Appl. Phys. Lett.* **1998**, *73*, 2441–2443.
(17) Qin, X.R.; Yang, D.; Frindt, R.F.; Irwin, J.C. *Phys. Rev. B* **1991**, *44*, 3490–3493.
(18) Pauling, L. *Proc. Natl. Acad. Sci. U.S.A.* **1929**, *15*, 709.
(19) Partin, D.E.; O'Keeffe, O. *J.Solid State Chem.* **1991**, *95*, 176–183.
(20) Leligny, H.; Monier, J.C. *Acta. Crystallogr. B* **1974**, *30*, 305.
(21) Leligny, H.; Monier, J.C. *Acta. Crystallogr. B.* **1975**, *31*, 728.
(22) Ramskar, M.; Skraba, Z.; Stadelmann, P.; Levy, F. *Adv. Mater.* **2000**, *12*, 814–818.
(23) Srolovitz, D.J.; Safran S.A.; Homyonfer M.; Tenne, R. *Phys. Rev. Lett.* 1995, 74, 1780–1782.
(24) Feldman, Y.; Frey, G.L.; Homyonfer, M.; Lyakhovitskaya, V.; Margulis, L.; Cohen, H.; Hodes, G.; Hutchison, J.L.; Tenne, R. *J. Am. Chem. Soc.* **1996**, 118, 5362–5367.
(25) Zak, A.; Feldman, Y.; Alperovich, V.; Rosentsveig, R.; Tenne, R. *J. Am. Chem. Soc.* **2000**, 122, 11108–11116.
(26) Ugarte, D., *Nature* **1992**, *359*, 707–709.
(27) Banhart, F.; Ajayan, P.J. *Nature* **1996**, 382, 433–435.
(28) José-Yacamán, M.; Lopez, H.; Santiago, P.; Galván, D.H.; Garzón I.L.; Reyes, A. *Appl. Phys. Lett.* **1996**, 69, 1065–1067.
(29) Galván, D.H.; Rangel, R.; Alonso, G. *Fullerene Sci. Tech.* **1998**, 1025–1035.
(30) Bates, K.R. and Scuseria, G.E. *Theor. Chem. Acc.* **1998**, 99, 29–33.